Available online at www.elixirpublishers.com (Elixir International Journal)

Vibrational Spectroscopy

Elixir Vib. Spec. 91 (2016) 38381-38391

ISSN: 2229-712X

Analysis of Vibrational Spectra of 2-Amino-5-Bromo-4-Methylpyridine Based on *Ab Initio* and Density Functional Theory Calculations

K.Sambathkumar

Department of Physics, A.A.Govt.Arts College, Villupuram-605602.India.

ARTICLE INFO

Article history:

Received: 1 January 2016;

Received in revised form: 5 February 2016;

Accepted: 11 February 2016;

Keywords

FTIR,
FT-Raman,
HOMO,
LUMO,
TED,
NMR,
ABMP.

ABSTRACT

Theoretical studies were conducted on the molecular structure and vibrational spectra of 2-amino-5-bromo-4-methylpyridine (ABMP). The FT-IR and FT-Raman spectra of ABMP were recorded in the solid phase. The molecular geometry and vibrational frequencies of ABMP in the ground state have been calculated by using the *ab initio* HF (Hartree-Fock) /6-311+G(d,p) and density functional methods (B3LYP) invoking 6-311+G(d,p)/6-311++G(d,p) basis set. The optimized geometric bond lengths and bond angles obtained by HF method show best agreement with the experimental values. Comparison of the observed fundamental vibrational frequencies of ABMP with calculated results by HF and density functional methods indicates that B3LYP is superior to the scaled Hartree-Fock approach for molecular vibrational problems. The difference between the observed and scaled wave number values of most of the fundamentals is very small. A detailed interpretation of the FT-IR and FT- Raman, NMR spectra of ABMP was also reported. NBO analysis has been performed in order to elucidate charge transfers or conjugative interaction, the intra-molecule rehybridization and delocalization of electron density within the molecule. UV–vis spectrum of the compound was recorded and the electronic properties, such as HOMO and LUMO energies, were performed by time dependent density functional theory (TD-DFT) approach. Finally the calculations results were applied to simulated infrared and Raman spectra of the title compound which show good agreement with observed spectra.

Introduction

The pyridine derivatives have an important position in the heterocyclic compounds and are important in bactericidal, fungicidal, germicidal and pharmacological activities [1]. And they can be used as nonlinear materials and photochemicals. Pyridines are widely used in pharmacological and medical applications. Some of them show anesthetic properties and have been used as drugs for certain brain diseases [2-4]. Pyridine tagged oligosaccharides have been widely used for sensitive qualitative and quantitative analysis by high performance liquid chromatography with fluorescence detection [2]. Pyridine is used in preparation of cytidine analogs [5] and it is also immensely used as a reagent in analytical chemistry. The vibrational spectra of 6-methyl pyridine have been investigated by several authors [6-9]. Extensive research in the last decade has shown that organic compounds often possess a higher degree of optical non-linearity than their inorganic counterparts. The literatures [10-12] supported by data banks [13-18] of various national and international journals an attempt has been made in this study to interpret the vibrational spectra of 2-amino-5-bromo-4-methylpyridine (ABMP) are performed by combining the experimental and theoretical information using density functional theory (B3LYP) and *ab initio* (HF) [19] to derive information about electronic effects and intramolecular charge transfer responsible for biological activity. The atomic charges, distribution of electron density (ED) in various bonding and antibonding orbitals and stabilisation energies, $E^{(2)}$ have been calculated by natural bond orbital (NBO) analysis. The NMR, HOMO-LUMO energy gap have been constructed at B3LYP/6-311++G(d,p) level to understand the electronic properties, electrophilic and nucleophilic active centres of MMP and ABMP.

Experimental and Computational Details

Experimental

The pure sample of 2-amino-5-bromo-4-methylpyridine (ABMP) was obtained from Lancaster Company, UK that is of spectroscopic grade and hence used for recording the spectra as such without any further purification. The FT-IR spectra of ABMP is measured in the BRUKER IFS 66V spectrometer in the range 4000 - 400 cm^{-1}. The FT-Raman spectrum of MMP and ABMP was also recorded in FT-RAMAN BRUKER RFS 100/S instrument equipped with Nd:YAG laser source operating at 1064 nm wavelength and 150 mW powers in the range 3500 - 50 cm^{-1}.

Tele:+91 9994188861.
E-mail addresses:a75kumar@yahoo.co.in

Computational

The initial geometry of ABMP was optimized using the *ab initio* (HF) and B3LYP of GAUSSIAN 09W program package [20]. The vibrational frequency analysis was computed using *ab initio* (HF/6-311+G(d,p)) and B3LYP/ 6-311+G(d ,p)/6-311++G(d,p) method to determine the nature of a stationary point found by geometry optimization. All the calculations such as first hyperpolarizability, HOMO–LUMO, NMR, NBO analysis were carried out by using B3LYP/6-311++G(d,p) method. It can be noted that the calculated frequencies are harmonic while the observed frequencies contain anharmonic contributions. The observed frequencies are generally lower than the calculated frequencies due to anharmonic nature of molecular vibrations. In principle, we should compare the calculated frequencies with experimental harmonic frequencies. However, as all the vibrations are more or less anharmonic, harmonic frequencies are not directly observable. Despite they can be deduced theoretically, it requires detailed knowledge of both quadratic and anharmonic force constants and is only feasible for every molecule. It should be pointed out that reproduction of observed fundamental frequencies is more desirable practically because they are directly observable in a vibrational spectrum. Therefore, comparison between the calculated and the observed vibrational spectra helps us to understand the observed spectral features. In order to improve the agreement of theoretically calculated frequencies with experimentally calculated frequencies, it is necessary to scale down the calculated frequencies by using the scale factors 0.914, 0.87, 0.99 and 1.07 for HF/6-311+G(d,p) and for B3LYP/6-311+G(d,p) set is scaled 0.955, 0.93, 1.01, 0.99, and 1.07 and B3LYP/6-311++G(d,p) basis set is scaled with 0.96, 0.947, 1.01, 1.07 and 0.99. Hence, the vibrational frequencies theoretically calculated at HF/6-311+G(d,p), B3LYP/6-311+G(d,p) and B3LYP/6-311++G(d,p) are scaled down by using MOLVIB 7.0 version written by Tom Sundius [21-23].

Results and Discussion

Geometrical parameters

The molecular structure ABMP belongs to C_1 point group symmetry. For C_1 symmetry there would not be any relevant distribution. The molecule consists of 18 and 16 atoms and expected to have 42 normal modes of vibration of the same (A) species under C_1 symmetry. The optimized structural parameters are calculated at *ab initio* (HF) 6-311+G(d,p) and DFT (B3LYP) levels with the 6-311+G(d,p)/6-311++G(d,p) basis set are listed in Tables 1 in accordance with the atom numbering scheme given in Fig.1, respectively for ABMP and the calculated geometrical parameters are compared with X-ray diffraction result. Detailed description of vibrational modes can be given by means of normal coordinate analysis. For this purpose, the full set of 53 standard internal coordinates (containing 11 redundancies) for ABMP are presented in Table 2. From these, a non-redundant set of local symmetry coordinates are constructed by suitable linear combinations of internal coordinates following the recommendations of Pulay and Fogarasi [24] which are presented in Table 3, respectively for ABMP. The experimentally and theoretically calculated IR, Raman frequencies are presented in Table 4 respectively for ABMP. The FT-IR and FT-Raman spectra of the ABMP are shown in Figs. 2,3.

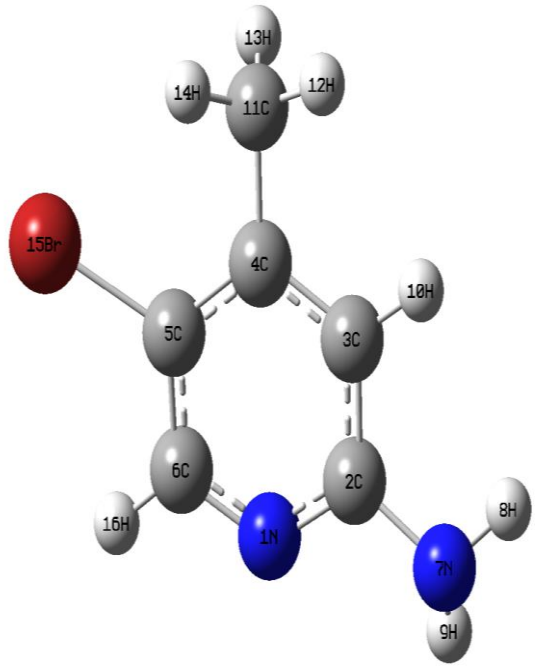

Figure 1. Molecular structure of 2-amino-5-bromo-4-methylpyridine

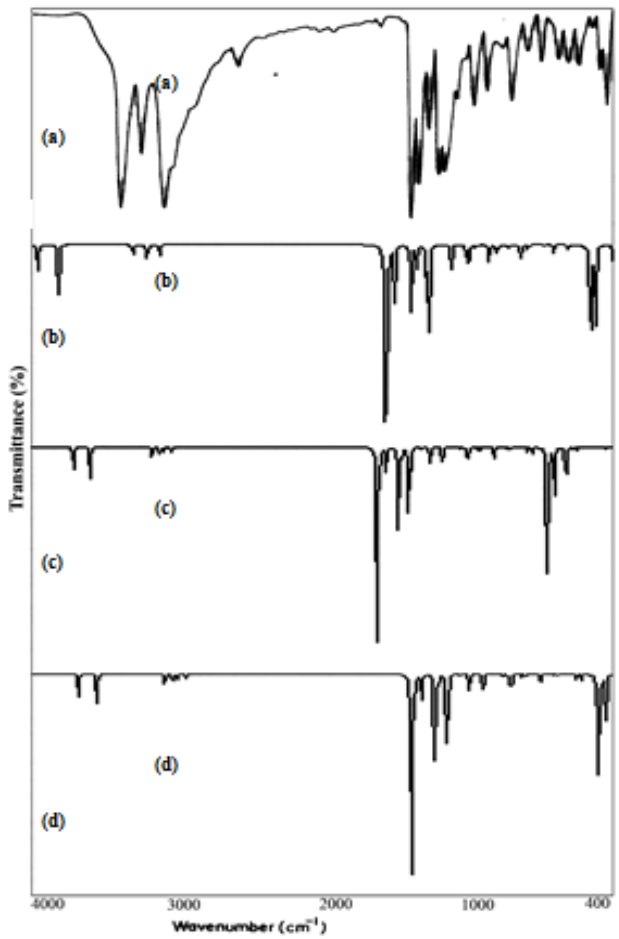

Fig 2. Observed and calculated IR spectrum of 2-amino-5-bromo-4-methylpyridine
(a) Observed
(b) HF/6-311+G(d,p)
(c) B3LYP/6-311+G(d,p)
(d) B3LYP/6-311++G(d,p)

Table 1. Optimized geometrical parameters of 2-amino-5-bromo-4-methylpyridine obtained by HF/6-31+G(d,p) and B3LYP/6-311G+(d,p) and 6-311++G(d,p) methods and basis set calculations

Bond Length	Value (Å)			Exp[a]	Bond Angle	Value (°)			Exp[a]	Dihedral Angle	Value (°)		
	HF/ 6-31+G(d,p)	B3LYP/ 6-311+G(d,p)	B3LYP/ 6-311++G(d,p)			HF/ 6-31+G(d,p)	B3LYP/ 6-311+G(d,p)	B3LYP/ 6-311++G(d,p)			HF/ 6-31+G(d,p)	B3LYP/ 6-311+G(d,p)	B3LYP/ 6-311++G(d,p)
N1-C2	1.3191	1.3375	1.3375	1.395	C2-C1-C6	118.095	117.94	117.94	123.6	C6-N1-C2-C3	-0.2325	-0.3137	-0.3062
N1-C6	1.3226	1.3339	1.3339	1.340	C1-C2-C3	122.35	122.29	122.29	118.5	C6-N1-C2-N7	177.903	177.47	177.47
C2-C3	1.4019	1.4065	1.4065	1.394	C1-C2-C7	116.76	116.37	116.37		C2-N1-C6-C5	0.3869	0.4119	0.4177
C2-H7	1.372	1.3812	1.3813		C3-C2-C7	120.85	121.29	121.29		C2-N1-C6-Br16	-179.84	-179.87	-179.88
C3-C4	1.3789	1.3901	1.3901	1.394	C2-C3-C4	119.88	120.23	120.23		N1-C2-C3-C4	-0.0619	-0.013	-0.0217
C3-H10	1.075	1.0848	1.0848		C2-C3-C10	119.83	120.05	120.05		N1-C2-C3-H10	179.35	179.49	179.45
C4-H5	1.3989	1.4046	1.4046	1.395	C4-C3-C10	120.26	119.7	119.7		C7-C2-C3-C4	-178.12	-177.69	-177.69
C4-C11	1.505	1.5033	1.5033		C3-C4-C5	116.68	116.32	116.32	118.1	C7-C2-C3-H10	1.2895	1.808	1.7812
C5-N6	1.3755	1.3878	1.3878	1.340	C3-C4-C11	120.69	120.90	120.90		N1-C2-N7-H8	156.55	157.10	156.99
C5-Br15	1.895	1.92	1.92		C5-C4-C11	122.61	122.76	122.77		N1-C2-N7-H9	15.705	15.705	15.7168
C6-H16	1.0748	1.0851	1.0851		C4-C5-C6	119.33	119.93	119.94	123.3	C3-C2-N7-H8	-25.299	-25.081	-25.2048
N7-H8	0.9937	1.0074	1.0074		C4-C5-Br15	121.63	121.37	121.36		C2-C3-N7-H9	-166.12	-166.48	-166.48
N7-N9	0.995	1.0091	1.0092		C6-C5-Br15	119.02	118.68	118.68		C2-C3-C4-C5	0.2049	0.2428	0.238
C11-H12	1.0825	1.0909	1.0909		N1-C6-C5	123.64	123.25	123.25		C2-C3-C4-C11	-179.94	-179.93	-179.932
C11-H13	1.0842	1.0934	1.0934		N1-C6-H16	116.24	116.50	116.50		H10-C3-C4-C5	-179.20	-179.26	-179.237
C11-H14	1.0842	1.0933	1.0933		C5-C6-H16	120.10	120.24	120.24		H10-C3-C4-H11	0.6472	0.5617	0.5924
					C2-N7-H8	117.76	118.06	118.04		C3-C4-C5-N6	-0.0654	-0.1537	-0.1364
					C2-N7-H9	114.94	114.84	114.81		C3-C4-C5-Br15	179.86	-179.99	-179.99
					H8-N7-H9	115.18	115.34	115.31		C11-C4-C5-C6	-179.91	-179.97	-179.96
					C4-C11-H12	110.60	110.88	110.88		C11-C4-C5-Br15	0.0144	0.1786	0.1809
					C4-C11-H13	110.69	110.92	110.91		C3-C4-C11-C12	0.0699	0.0562	0.0248
					C4-C11-H14	110.68	110.89	110.89		C3-C4-C11-C13	120.59	120.811	120.78
					H12-C11-H13	108.68	108.60	108.60		C3-C4-C11-C14	-120.42	-120.65	-120.69
					H12-C11-H14	108.66	108.58	108.58		C5-C4-C11-C12	179.91	179.87	179.84
					H13-C11-H14	107.40	106.82	106.82		C5-C4-C11-C13	-59.563	-59.374	-59.40
										C5-C4-C11-C14	59.416	59.158	59.125
										C4-C5-C6-C1	-0.2396	-0.1791	-0.1979
										C4-C5-C6-C16	-179.99	-179.88	-179.88
										Br15-C5-C6-C1	179.83	179.67	179.66
										Br15-C5-C6-H16	0.0715	-0.0357	-0.0261

For numbering of atom refer Fig. 1.
[a] Value taken from Ref [33]

Table 2. Definition of internal coordinates of 2-amino-5-bromo-4-methylpyridine

No. (i)	Symbol	Type	Definition[a]
Stretching			
1 – 2	R_i	C-H	C3-H10, C6-H6
3	Q_i	C-Br	C5-Br15
4-6	q_i	C-N	C2-N1, C6-N1, C2-N7
7-11	P_i	C-C	C2-C3, C3-C4, C4-C5, C5-C6, C4-C11
12-14	r_i	C-H methyl	C11-H12, C11-H13, C11-H14
15-16	q_i	N-H_2	N7-H8, N7-H9
In-plane bending			
17 - 22	α_i	ring	N1-C2-C3, C2-C3-C4, C3-C4-C5, C4-C5-C6, C5-C6-N1, C6-N1-C2
23 - 25	β_i	C-C-H	C4-C11-H12, C4-C11-H14, C4-C11-H13
26-28	σ_i	H-C-H	H12-C11-H14, H12-C11-H13, H13-C11-H14
29-30	ν_i	C-C-C	C3-C4–C11, C5-C4–C11
31- 33	Z_i	C-C-H	C2-C3-H10, C4-C3-H10, C5-C6-H16
34	ν_i	N-C-H	N1-C6-H16
35	ε_i	N-C-N	N1-C2-N7
36,37	δ_i	N-C-Br	C4-C5-Br15, C6-C5-Br15
38,39	η_i	C-N-H	C2-N7-H9, C2-N7-H8
40	ψ_i	H-N-H	H8-N7-H9
Out-of-plane bending			
41-42	θ_i	C-H	H10-C3-C2-C4, H16-C6-N1-C5
43	ρ_i	C-C	C11-C4-C3-C5
44	χ_i	N-C	N7-C2-N1-C3
45	ω_i	C-Br	Br15-C5-C4-C6
Torsion			
46-51	τ_i	tRing	N1-C2-C3-C4, C2-C3-C4-C5, C3-C4-C5-C6, C4-C3-C6-N1, C5-C6-N1-C2, C6-N1-C2-C3
52	τ_i	tC-NH_2	C2-N7-H9-H8
53	τ_i	tC-CH_3	(C5,C3)-C4-C11-(H12,H13,H14)

[a] For numbering of atoms refer Fig. 1.

Table 3. Definition of local symmetry coordinates of 2-amino-5-bromo- 4-methylpyridine.

No. (i)	Type	Definition[b]
1-2	C H	R_1, R_2
3	CBr	Q_6
4-6	CN	q_7, q_8, q_9
7-11	CC	P_7, P_8, P_9, P_{10}, P_{11}
12	CH_3 ss	$(r_{13} + r_{14} + r_{15}) / \sqrt{3}$
13	CH_3 ass	$(2r_{13} + r_{14} + r_{15}) / \sqrt{6}$
14	CH_3 ops	$(r_{14} - r_{15}) / \sqrt{6}$
15	NH_2ss	$(q_{19} + q_{20}) / \sqrt{2}$
16	NH_2ips	$(q_{19} - q_{20}) / \sqrt{2}$
17	R trigd	$(\alpha_{17} - \alpha_{18} + \alpha_{19} - \alpha_{20} + \alpha_{21} - \alpha_{22}) / \sqrt{6}$
18	R symd	$(-\alpha_{17} - \alpha_{18} + 2\alpha_{19} - \alpha_{20} - \alpha_{21} + 2\alpha_{22}) / \sqrt{12}$
19	R asymd	$(\alpha_{17} - \alpha_{18} + \alpha_{20} - \alpha_{21}) / \sqrt{2}$
20	CH_3 sb	$(-\beta_{23} - \beta_{24} - \beta_{25} + \sigma_{26} + \sigma_{27} + \sigma_{28}) / \sqrt{2}$,
21	CH_3 ipb	$(\sigma_{26} - \sigma_{27} - 2\sigma_{28}) / \sqrt{6}$
22	CH_3 opb	$(-\sigma_{26} + \sigma_{27}) / \sqrt{2}$
23	CH_3 ipr	$(2\beta_{23} - \beta_{24} - \beta_{25}) / \sqrt{6}$
24	CH_3 opr	$(\beta_{24} - \beta_{25}) / \sqrt{2}$
25	b CC	$(\nu_{29} - \nu_{30}) / \sqrt{2}$
26,27	b CH	$(Z_{31} - Z_{32}) / \sqrt{2}$, $(Z_{33} - \upsilon_{34}) / \sqrt{2}$
28	b CN	$(\varepsilon_{35}) / \sqrt{2}$
29	b CBr	$(\delta_{36} - \delta_{37}) / \sqrt{2}$
30	NH_2rock	$(\eta_{38} - \eta_{39}) / \sqrt{2}$
31	NH_2twist	$(\eta_{38} + \eta_{39}) / \sqrt{2}$
32	NH_2sciss	$(2\psi_{40} - \eta_{39} - \eta_{38}) / \sqrt{2}$
33,34	ω C H	θ_{41}, θ_{42}
35	ω CC	ρ_{43}
36	ω NC	χ_{44}
37	ω NBr	ω_{45}
38	tRtrigd	$(\tau_{46} - \tau_{47} + \tau_{48} - \tau_{49} + \tau_{50} - \tau_{51}) / \sqrt{6}$
39	tRsymd	$(\tau_{46} - \tau_{48} + \tau_{49} - \tau_{51}) / \sqrt{2}$
40	tRasymd	$(-\tau_{46} + 2\tau_{47} - \tau_{48} - \tau_{49} + 2\tau_{50} - \tau_{51}) / \sqrt{12}$
41	τN-NH_2	τ_{52}, τ_{53}
42	τC-CH_3	τ_{54}

[b] The internal coordinates used here are defined in Table 2.

Table 4. The observed (FTIR and FT-Raman) and calculated (unscaled and scaled) fundamental harmonic frequencies (cm^{-1}), of 2-amino-5-bromo-4-methylpyridine are analysed based on SQM force field calculation using HF/6-311+G(d,p), B3LYP/6-311+G(d,p) and B3LYP/6-311++G(d,p) method and basis set calculations

Observed frequencies		Calculated frequency (cm^{-1}) with HF/6-311+G(d,p)		Calculated frequency (cm^{-1}) with B3LYP/ 6-311+G(d,p)		Calculated frequency (cm^{-1}) with B3LYP/ 6-311++G(d,p)		Assignments (TED %)
FTIR	FT-Raman	Unscaled	Scaled	Unscaled	Scaled	Unscaled	Scaled	
3493(vs)	-	3949	3772	3696	3490	3696	3495	NH2ass(99)
3390(s)	3391(vs)	3924	3676	3599	3388	3585	3392	NH2ass(98)
3110(s)	-	3872	3512	3469	3371	3469	3114	υCH(97)
-	3101(vs)	3758	3462	3364	3330	3164	3104	υCH(95)
2887(w)	-	3682	3588	3345	3310	3115	2889	CH3ss(96)
-	2773(w)	3566	3473	3288	3271	3088	2775	CH3ips(94)
2215(s)	2213(w)	3200	3190	3035	3003	3035	2218	CH3ops(90)
-	1690(w)	1904	1856	1746	1705	1701	1696	υCC(77), CH3ss(21)
1681(w)	-	1887	1840	1734	1723	1699	1683	υCC(67), CH3ips(23), CH3ops, (9)
1674(vw)		1851	1810	1722	1705	1682	1675	υCC(61),CH3ops(17),CH3ss(12), υCN(10)
-	1662(vw)	1841	1801	1712	1706	1699	1666	υCC(60), υCN(23), CH3ops(12)
1642(s)	-	1814	1799	1685	1672	1785	1644	υCC(65),υCN(24), CH3ips(11)
-	1612(s)	1808	1757	1678	1664	1778	1617	NH2sisc(56),υCC(21),υCN(14),NH2sisc(9)
1496(w)	-	1754	1730	1666	1656	1730	1499	υCN(59),υCC(19),NH2sisc(15),CH3ipr(11)
-	1492(s)	1736	1723	1655	1641	1715	1494	υCN(57),CH3ipb(18),CH3opr(14), υCC(10)
-	1414(w)	1689	1678	1648	1613	1638	1419	υCN(55),CH3sb(25),CH3ipr(13), υCC(9)
1393(s)	1395(w)	1678	1667	1629	1601	1623	1397	CH3ipb(52), υCN(27),υCC(12), CH3ipr(8)
1387(w)	1388(w)	1665	1598	1611	1589	1612	1398	CH3sb(53), bCH(20), υCC(16), υCN(11)
1252(w)	-	1654	1578	1601	1567	1604	1257	bCH(50), CH3ipr(32),CH3opr(17)
1243(w)	-	1625	1564	1578	1556	1586	1249	bCH(56), CH3opr(22),NH2rock(13)
1202(w)	1200(w)	1612	1556	1572	1534	1574	1209	CH3opb(62), bCH(21),Rtrigd(17)
-	1170(w)	1607	1546	1535	1523	1535	1174	NH2rock(68), Rtrigd(16),bCC(14)
1142(w)	1141(w)	1599	1534	1523	1514	1524	1148	CH3opr(59), Rsymd(20),NH2 wag(9)
991(w)	993(w)	1306	1291	1288	1267	1224	997	CH3ipr(55), Rasymd(25),NH2rock(15)
-	881(w)	1047	1023	1009	991	1301	887	bCC(59), NH2wag(19),Rsymd(12)
874(w)	-	1001	989	982	967	1278	879	Rtrigd(53), NH2rock(24), bCN(19)
-	861(w)	999	987	970	960	1267	868	Rsymd(51), bCH(20),bCN(17), ωCH(11)
-	850(w)	991	978	947	913	999	859	NH2wag(49), bCH(21), Rasymd(17), υCBr(13)
-	842(vw)	979	960	931	912	978	847	Rasymd(61), bCC(13), bCBr(10), ωCH(8)
-	768(w)	968	950	923	860	961	777	bCN(55), ωCC(26), bCBr(18)
645(w)	-	956	944	921	840	846	652	ωCH(51), υCBr(22), tRtrigd(18), bCBr(9)
633(w)	-	945	902	896	829	834	639	ωCH(44), bCN(25), tRsymd(21), ωCC(10)
-	610(w)	816	757	676	657	824	617	ωCC(58), ωCH(28), tRasymd(14)
528(w)	-	800	789	648	620	814	532	υCBr(67), ωCH(32)
-	512(w)	789	747	671	610	790	523	bCBr(69), tRtrigd(23)
507(w)	-	675	644	623	604	588	519	tRtrigd(59), ωCH(20), tRasymd(17)
-	503(w)	651	612	594	580	564	515	tRsymd(56), bCBr(27), tRtrigd(12)
497(w)	-	693	608	568	493	534	508	tRasymd(53), ωCN(27), tRsymd(19)
-	310(w)	678	632	541	530	512	317	NH2 twist(57), ωCBr(13), ωCN(9)
-	210(w)	666	634	596	507	499	218	ωCN(50), NH2 twist(32), ωCBr(16)
-	152(w)	567	467	431	399	380	159	ωCBr(51), tRasymd(29), NH2 twist(17)
-	101(w)	421	389	329	294	192	110	tCCH3(59)

Abbreviations: ν - stretching; b - in-plane bending; ω - out-of-plane bending; asymd - asymmetric; symd - symmetric; t - torsion; trig - trigonal; w - weak; vw - very week; vs - very strong; s - strong; ms - medium strong; ss - symmetric stretching; ass - asymmetric stretching; ips - in-plane stretchingj; ops - out-of-plane stretching; sb - symmetric bending; ipr - in-plane rocking; opr - out-of-plane rocking; opb - out-of-plane bending.

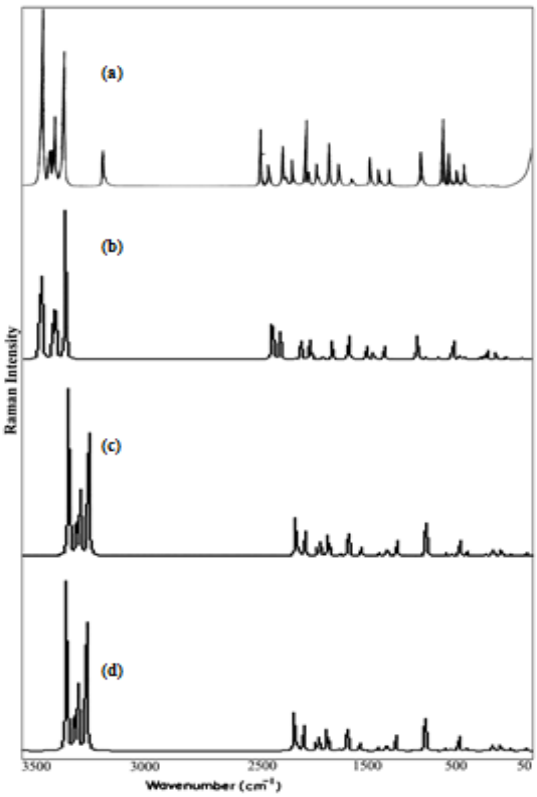

Figure 3.Observed and calculated Raman spectrum of 2-amino-5-bromo- 4-methylpyridine
(a) Observed
(b) HF/6-311+G(d,p)
(c) B3LYP/6-311+G(d,p)
(d) B3LYP/6-311++G(d,p)

C-H vibrations

The hetero aromatic structure shows the presence of C-H stretching vibration in the region 3100-3000 cm^{-1} which is the characteristic region for the identification of such C-H stretching vibrations. These vibrations are not found to be affected due to the nature and position of the substituents. In the present investigation, the C–H vibrations are observed at 3151 cm^{-1} in the FTIR spectrum and at 3110 cm^{-1} and 3101 cm^{-1} in the FTIR and FT-Raman spectra for ABMP, respectively. The C-H in-plane-bending vibrations usually occur in the region 1390-990 cm^{-1} and are very useful for characterization purposes. Substitution patterns on the ring can be judged from the out-of-plane bending vibrations occur in the region 900-675 cm^{-1} and these bands are highly informative [25]. Therefore, the IR peaks observed at 1252, 1243 cm^{-1} in the ABMP have been assigned to, C-H in-plane-bending vibrations. The C-H out-of-plane bending vibrations are observed at 645, 633 cm^{-1} in the FTIR spectrum for ABMP.

C-C vibrations

The C-C heteroaromatic stretching vibrations are occurring near 1650-1400 cm^{-1} are good group vibrations [25]. With heavy substituents, the bonds tend to shift to somewhat lower wavenumbers and greater the number of substituents on the ring, broader the absorption regions. As predicted in the earlier references, in the present investigation, the C–C stretching vibrations observed at 1681, 1674, 1642 cm^{-1} in FT-IR and 1690, 1662 cm^{-1} in FT-Raman for ABMP, are confirmed by their TED values. Most of the ring vibrational modes are affected by the substitutions in the hetero aromatic ring of ABMP. In the present study, the bands are observed at 881 cm^{-1} in Raman for ABMP, have been designated to ring in-plane bending modes by careful consideration of their quantitative descriptions. The ring out-of-plane bending modes of ABMP are also listed in Table 4, respectively.

C-N vibrations

In hetero aromatic compounds, the C-N stretching vibrations usually lies in the region 1400 - 1200 cm^{-1}. The identification of C-N stretching frequencies is a rather difficult task. Since the mixing of vibrations is possible in this region [25]. The IR and Raman bands found at 1496 cm^{-1} and 1492, 1414 cm^{-1} have been assigned to C–N stretching vibrations of ABMP. The C–N bending vibrations and deformations are in close agreement with literature value and also supported the TED values.

C-Br Vibrations

The vibrations that are belonging to the bond between the ring and the halogen atoms are worth to discuss here, since mixing of vibrations are possible due to the presence of heavy atoms on the periphery of the compound [175]. C-X bond show lower absorption frequencies as compared to C-H bond due to the decreased force constant and increase in reduced mass. Further, Br causes redistribution of charges in the ring. Bromine compounds absorbed in the region 650-485cm^{-1}due to the C-Br stretching vibrations. In ABMP, C-Br stretching vibrations are observed at 528 cm^{-1}in the IR spectrum, and the Raman spectrum, the peaks are observed at 512 cm^{-1} for ABMP have been assigned to C-Br in-plane-bending vibrations. The observed C-H out-of-plane bending modes show consistent agreement with the computed B3LYP method.

CH_3 group vibrations

The investigated molecule under consideration possesses CH_3 groups in fourth position of ABMP. For the assignments of CH_3 group frequencies one can expected that nine fundamentals can be associated to each CH_3 group, namely three stretching, three bending, two rocking modes and a single torsional mode describe the motion of methyl group. The above modes are defined in Table 4. The CH_3 symmetric stretching frequency is identified at 2887 cm^{-1} in the FTIR spectrum for ABMP. The CH_3 in-plane stretching vibrations are identified at 2773 cm^{-1} in FT-Raman spectrum for ABMP. The CH_3 symmetric bending and CH_3 in-plane bending frequencies are attributed at 1393, 1387 cm^{-1} in the FTIR and at 1395, 1388 cm^{-1} FT-Raman spectrum for ABMP. These assignments are supported by literature [25]. The in-plane rocking and out-of-plane rocking modes of CH_3 group are found at 991 cm^{-1} and 1142 cm^{-1} in the FTIR and at 993 cm^{-1} and 1141 cm^{-1} FT-Raman spectrum for ABMP. The bands obtained at 2490, 2481 cm^{-1} and 1190, 1185 cm^{-1} in the FTIR spectrum and at 2215, 1202 cm^{-1} in the FTIR and at 2213, 1200 cm^{-1} FT-Raman spectrum for ABMP assigned to CH_3 out-of-plane stretching and CH_3 out-of-plane bending modes, respectively. The assignment of the bands at 101 cm^{-1} FT-Raman spectrum for ABMP attributed to methyl twisting mode.

NH_2 vibrations

The molecule under consideration possesses NH_2 group and hence six internal modes of vibration are possible such as symmetric stretching, asymmetric stretching, scissoring, rocking, wagging and torsional mode for ABMP respectively. The frequency of asymmetric vibration is higher than that of symmetric one. The frequencies of amino group in the region

3500 - 3300 cm^{-1} for NH stretching, 1700 - 1600 cm^{-1} for scissoring and 1150 - 900 cm^{-1} for rocking deformation [25]. In the present investigation, the asymmetric and symmetric stretching modes of NH_2 group are assigned at 3493 cm^{-1} in FTIR and 3390 cm^{-1} in FTIR and 3391 cm^{-1} in FT-Raman spectrum respectively. The band observed at 1612 cm^{-1} in FT-Raman spectrum is assigned to NH_2 scissoring mode. The rocking, wagging, twisting deformation vibrations of NH_2 contribute to several normal modes in the low frequency region. The band observed at 1170 cm^{-1} in Raman is assigned to NH_2 rocking vibrations and the FT-Raman band observed at 850 cm^{-1} is assigned to NH_2 wagging modes, and the band observed at 310 cm^{-1} in Raman is assigned to NH_2 twisting modes [25].

Prediction of Non-Linear Optical Properties

The first hyperpolarizability (β_0) of this novel molecular system and the related properties (β_0, α_0) of ABMP are calculated using the HF/6-311+G(d,p) and B3LYP/6-311++G(d,p) basis set, based on the finite field approach. In the presence of an applied electric field, the energy of a system is a function of the electric field. The first hyperpolarizability is a third-rank tensor that can be described by a $3 \times 3 \times 3$ matrix. The 27 components of the 3D matrix can be reduced to 10 components due to the Kleinman symmetry [26]. It can be given in the lower tetrahedral. The components of β are defined as the coefficients in the Taylor series expansion of the energy in the external electric field. When the external electric field is weak and homogenous, this expansion becomes:

$$E = E_0 - \mu_\alpha F_\alpha - 1/2\alpha_{\alpha\beta}F_\alpha F_\beta - 1/6\beta_\alpha\beta_\gamma F_\alpha F_\beta F_\gamma + ...$$

where E_0 is the energy of the unperturbed molecules, F_α the field at the origin and μ_α, $\alpha_{\alpha\beta}$ and $\beta_\alpha\beta_\gamma$ are the components of dipole moment, polarizability and the first hyperpolarizabilities, respectively. The total static dipole moment μ, the mean polarizability α_0 and the mean first hyperpolarizability β_0, using the x, y, z components they are defined as

$$\mu = (\mu_x^2+\mu_y^2+\mu_z^2)^{1/2}$$
$$\alpha_0 = (\alpha_{xx}+\alpha_{yy}+\alpha_{zz})/3$$
$$\alpha = 2^{-1/2}[(\alpha_{xx}-\alpha_{yy})^2 + (\alpha_{yy}-\alpha_{zz})^2 + (\alpha_{zz}-\alpha_{xx})^2 + 6\alpha_{xx}^2)^{1/2}$$
$$\beta_0 = (\beta_x^2+\beta_y^2+\beta_z^2)^{1/2}$$
$$\beta_{vec} = 3/5[(\beta_x^2+\beta_y^2+\beta_z^2)^{1/2}]$$

where

$$\beta_x = \beta_{xxx} + \beta_{xyy} + \beta_{xzz}$$
$$\beta_y = \beta_{yyy} + \beta_{yxx} + \beta_{yzz}$$
$$\beta_z = \beta_{zzz} + \beta_{zxx} + \beta_{zyy}$$

The β_0 components of GAUSSIAN 09W program package output are reported in atomic units and therefore the calculated values are converted into e.s.u. units (1 a.u. = 8.3693×10^{-33} e.s.u.). The calculated value of hyperpolarizability and polarizability of ABMP are tabulated in Table 5. We can conclude that the title molecules are an attractive object for future studies of non-linear optical properties.

Homo-Lumo Analysis

This electronic absorption corresponds to the transition from the ground to the first excited state and is mainly described by one electron excitation from the highest occupied molecular orbital (HOMO) to the lowest unoccupied molecular orbital (LUMO) [25,26]. Many organic molecule, containing conjugated π electrons are characterized by large values of molecular first hyper polarizabilities, are analyzed by means of vibrational spectroscopy. In most of the cases, even in the absence of inversion symmetry, the strongest band in the Raman spectrum is weak in the IR spectrum and vice-versa. But the intra molecular charge from the donor to acceptor group through a single-double bond conjugated path can induce large variations of both the molecular dipole moment and the molecular polarizability, making IR and Raman activity strong at the same time. The analysis of the wave function indicates that the electron absorption corresponds to the transition from the ground to the first excited state and is mainly described by one-electron excitation from the highest occupied molecular orbital (HOMO) to the lowest unoccupied orbital (LUMO). In

Table 5. Nonlinear optical properties of 2-amino-5-bromo-4-methylpyridine calculated at HF/6-311++G(d,p) with B3LYP/6-311+G(d,p) and 6-311++G(d,p) method and basis set calculations

NLO behaviour	HF/ 6-311+G(d,p)	B3LYP/ 6-311+G(d,p)	B3LYP/ 6-311++G(d,p)
Dipole moment (μ)	0.7372 Debye	1.2195 Debye	1.5799 Debye
Mean polarizability (α)	0.8325×10^{-30} esu	0.9314×10^{-30} esu	0.9346×10^{-30} esu
Anisotropy of the polarizabilty (Δ_α)	1.0530×10^{-30} esu	1.1681×10^{-30} esu	2.4044×10^{-30} esu
First hyperpolarizability (β)	2.2104×10^{-30} esu	3.9039×10^{-30} esu	2.1918×10^{-30} esu
Vector-first hyperpolarizability (β_{vec})	1.3262×10^{-30} esu	2.3423×10^{-30} esu	1.3150×10^{-30} esu

Table 6. HOMO-LUMO energy gap and related molecular properties of 2-methoxy-6-methylpyridine and 2-amino-5-bromo-4-methylpyridine

Molecular Properties	B3LYP/6-311++G(d,p)
HOMO	**-0.2249**
LUMO	**-0.0378**
Energy gap	**0.1871**
Ionisation Potential (I)	**0.2249**
Electron affinity (A)	**0.0378**
Global softness (s)	**10.6894**
Global Hardness (η□)	**0.09355**
Chemical potential (μ)	**-0;1313**
Global Electrophilicity (ω)	**0.09208**

ABMP, the HOMO is located over heterocyclic ring and the HOMO-LUMO transition implies an electron density transfer to the CH_3, Br group from heterocyclic ring and oxygen atom, whereas in ABMP the HOMO is located over heterocyclic ring, especially on amino and oxygen atom, and the HOMO-LUMO transition implies an electron density transfer to the heterocyclic ring from amino group and oxygen atom. Moreover, the compositions of HOMO and LUMO for ABMP are shown in Fig. 4, respectively. The HOMO-LUMO energy gap of ABMP were calculated at B3LYP/6-311++G(d,p) level, which reveals that the energy gap reflects the chemical activity of the molecules. The LUMO as an electron acceptor (EA) represents the ability to obtain an electron donor (ED) and HOMO represents ability to donate an electron donor (ED). The ED groups to the efficient EA groups through □-conjugated path. The strong charge transfer interaction through □-conjugated bridge results in substantial ground state Donor-Acceptor (DA) mixing and the appearance of a charge transfer band in the electron absorption spectrum. The HOMO-LUMO energy gap explains the fact that eventual charge transfer interaction is taking place within the investigated molecules.

Global and local reactivity descriptors

Based on density functional descriptors global chemical reactivity descriptors of compounds such as hardness, chemical potential, softness, electronegativity and electrophilicity index as well as local reactivity have been defined [25-27]. Pauling introduced the concept of electronegativity as the power of an atom in a compound to attract electrons to it. Hardness (η), chemical potential (μ) and electronegativity (χ) and softness are defined follows.

$\eta = ½(\partial^2E/\partial N^2)_{V(r)} = ½(\partial\mu/\partial N)_{V(r)}$

$\mu = (\partial E/\partial N)_{V(r)}$

$\chi = -\mu = -(\partial E/\partial N)_{V(r)}$

where E and V(r) are electronic energy and external potential of an N-electron system respectively. Softness is a property of compound that measures the extent of chemical reactivity. It is the reciprocal of hardness.

$$S = 1/\eta$$

Using Koopman's theorem for closed-shell compounds, η, μ and χ can be defined as

$\eta = (I-A)/2$

$\mu = -(I+A)/2$

$\chi = (I+A)/2$

where A and I are the ionization potential and electron affinity of the compounds respectively. Electron affinity refers to the capability of a ligand to accept precisely one electron from a donor. However in many kinds of bonding viz. covalent hydrogen bonding, partial charge transfer takes places. Recently Parr *et al.* [28] have defined a new descriptor to quantity the global electrophilic power of the compound as electrophilicity index (ω), which defines a quantitative classification of the global electrophilic nature of a compound have proposed electrophilicity index (ω) as a measure of energy lowering due to maximal electron flow between donor and acceptor. They define electrophilicity index (ω) as

$\omega = \mu^2/2\eta$

The usefulness of this new reactivity quantity has been recently demonstrated in understanding the toxicity of various pollutants in terms of their reactivity and site selectivity [29-31]. The calculated value of electrophilicity index describes the biological activity for ABMP respectively. All the calculated values of HOMO-LUMO, energy gap, ionization potential, Electron affinity, hardness, potential, softness and electrophilicity index are shown in Table 6.

NBO Analysis

The NBO analysis is carried out by examining all possible interactions between 'filled' (donor) Lewis-type NBOs and 'empty' (acceptor) non-Lewis NBOs, and estimating their energetic important by 2nd order perturbation theory. Since these interactions lead to loss of occupancy from the localized NBOs of the idealized Lewis structure into the empty non-Lewis orbitals, they are referred to as delocalization corrections to the zeroth-order natural Lewis structure. For each donor NBO (i) and acceptor NBO (j) with delocalization $i \rightarrow j$ is estimated as

$$E^{(2)} = \Delta E_{ij} = q_i \frac{F(i,j)^2}{\varepsilon_j - \varepsilon_i}$$

where q_i is the donor orbital occupancy ε_j and ε_i are diagonal elements orbital energies and F(i, j) is the off diagonal NBO Fock matrix element. The larger $E^{(2)}$ value, the more intensive is the interaction between electron donors and acceptors, i.e., the more donation tendency from electron donors to electron acceptors and the greater the extent of conjugation of the whole system. DFT (B3LYP/6-311++G(d,p)) level computation is used to investigate the various second-order interactions between the filled orbitals of one subsystem and vacant orbitals of another subsystem, which is a measure of the delocalization or hyper-conjugation [27]. NBOs are localized electron pair orbitals for bonding pairs and lone pairs. The hybridization of the atoms and the weight of each atom in each localized electron pair bond are calculated in the idealized Lewis structure. A normal Lewis structure would not leave any antibonding orbitals, so the presence of antibonding orbitals shows deviations from normal Lewis structures. Anti bonding localized orbitals are called non-Lewis NBOs. In order to study the small deviations from idealized Lewis structure, the Donor–Acceptor interaction approach is adopted. In ABMP, π(C5-C6) → π*(C3-C4) interaction is seen to give a strong stabilization 54.01 kJ/mol. This strong stabilization denotes the larger delocalization. The interesting interactions in ABMP molecule are LP1N7, LP3Br15 with that of antibonding N1-C2, C5-C6. These two interactions result the stabilization energy of 39.91, 19.83 kJ/mol respectively. This highest interaction around the ring can induce the large bioactivity in the molecule. This shows that the lone pair orbital participates in electron donation in the molecule. The calculated values of $E^{(2)}$ are shown in Table 7 ABMP, respectively.

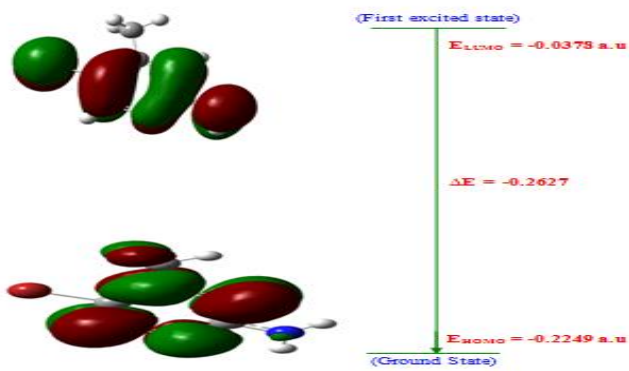

Figure 4. HOMO-LUMO Plot of 2-amino-5-bromo-4-methylpyridine

Table 7. Second-order perturbation theory analysis of Fock matrix in NBO basis of 2-amino-5-bromo-4-methylpyridine using DFT/B3LYP/6-311++G(d,p)basis set

Donor(i)	Type	ED/e	Acceptor(j)	Type	ED/e	$E^{(2)a}$(kJ/mol)	E(j)-E(i)[b] (a.u)	F(i,j)[c](a.u)
N1-C2	π	0.8556	C3-C4	π^*	0.2200	22.8028	0.33	0.054
N1-C2	π		C5-C6	π^*		59.5901	0.31	0.085
C2-C3	σ	0.9898	C4-C11	σ^*	0.0157	7.6148	1.09	0.056
C3-C4	σ	0.9824	C4-C5	σ^*	0.0110	9.1629	1.27	0.067
C3-C4	σ		C5-Br15	σ^*		11.7570	0.80	0.060
C3-C4	π	0.8369	N1-C2	π^*	0.1614	60.7098	0.26	0.080
C3-C4	π		C5-C6	π^*		33.3046	0.27	0.059
C3-H10	σ	0.9890	N1-C2	σ^*	0.0072	9.5395	1.06	0.062
C3-H10	σ		C4-H5	σ^*		8.4098	1.10	0.060
C5-C6	π	0.8400	N1-C2	π^*	0.1808	27.6144	0.27	0.055
C5-C6	π		C3-C4	π^*		54.0154	0.30	0.078
C6-H16	σ	0.9913	N1-C2	σ^*	0.0112	8.8282	1.06	0.060
N7-H8	σ	0.9928	N1-C2	σ^*	0.0019	8.5772	1.17	0.062
C11-H14	σ	0.9873	C3-C4	π^*	0.0035	9.0374	0.54	0.047
N1	LP(1)	0.9502	C2-C3	σ^*	0.0032	20.0832	0.88	0.084
N1	LP(1)		C2-N7	σ^*		9.4976	0.66	0.050
N1	LP(1)		C5-C6	σ^*		17.4054	0.87	0.077
N7	LP(1)		N1-C2	π^*		39.9153	0.33	0.077
Br15	LP(3)	0.9704	C5-C6	σ^*	0.0001	19.8321	0.30	0.052
N1-C2	π^*		C3-C4	π^*		309.2394	0.02	0.084
C5-C6	π^*		C3-C4	π^*		318.7371	0.02	0.080

[a] $E^{(2)}$ means energy of hyper conjugative interaction (stabilization energy).
[b] Energy difference between donor and acceptor i and j NBO orbitals.
[c] F(i, j) is the Fork matrix element between i and j NBO orbitals.

Table 8. The calculated shifts of carbon and hydrogen atoms of 2-amino-5-bromo-4-methylpyridine using B3LYP/6-311++G(d,p) GIAO method

Atom position	Isotropic chemical shielding tensor(σ)(ppm)	Chemical shifts(δ) (ppm)		
		Theoretical	Expt[a]	Δ
N1	-60.9321	319.332		
C2	13.6642	158.801	152.60	-11.201
C3	64.2451	118.221	105.32	-7.901
C4	28.9526	143.513	118.04	-5.473
C5	48.9346	123.531	145.75	-21.781
C6	31.5196	140.946	156.32	-40.626
N7	180.2596	78.1404		
H8	28.9900	28.99		
H9	29.4642	29.4642		
H10	25.4426	25.4426		
C11	157.8617	24.6039	22.26	-2.343
H12	29.8866	29.8866		
H13	29.7247	29.7247		
H14	29.3506	29.3506		
H16	23.8295	23.8295		

[a] Taken from Ref [34] and Δ (δ_{exp}-δ_{the}); difference between respective chemical shifts.

^{13}c and ^{1}h Nmr Spectral Analysis

The molecular structure of ABMP is optimized by using B3LYP method with 6-31++G(d,p) basis set. Then, GIAO ^{13}C calculations of the title compound are calculated and compared with experimental values [32] are shown in Table 8. Relative chemical shifts are then estimated by using the corresponding TMS shielding calculated in advance at the theoretical level as reference. Changes in energy needed to flip protons are called chemical shifts. The location of chemical shifts (peaks) on a NMR spectrum are measured from a reference point that the hydrogens in a standard reference compound —$(CH_3)_4S_i$ or tetramethylsilane (TMS)—produce. The amount of energy necessary to flip protons in TMS is assigned the arbitrary value of zero δ. Chemical shifts are measured in parts per million magnetic field strength difference (δ-scale), relative to TMS. The experimental values of ABMP for ^{1}H and ^{13}C isotropic chemical shielding for TMS were 159.38, 157.86 ppm, respectively [32]. All the calculations are performed using GAUSSVIEW molecular visualization program and Gaussian 09W program package. The result shows that the range ^{13}C NMR chemical shift of the typical organic compound usually is > 100 ppm [85,86], the accuracy ensures reliable interpretation of spectroscopic parameters. In practice, it is easier to fix the radio wave frequency and vary the applied magnetic field than it is to vary the radio wave frequency. The magnetic field "felt" by a hydrogen atom is composed of both applied and induced fields. The induced field is a field created by the electrons in the bond to the hydrogen and the electrons in nearby π bonds. When the two fields reinforce each other, a smaller applied field is required to flip the proton. In this situation, a proton is said to be deshielded. When the applied and induced fields oppose each other, a stronger field must be applied to flip the proton. In this state, the proton is shielded. Electronegative atoms such as Br, O_2, NH_2 and halogens deshield hydrogens. The extent of deshielding is proportional to the electronegativity of the heteroatom and its proximity to the hydrogen. Electrons have an heterocyclic ring, double bonded atoms, and triple bonded atoms deshield attached hydrogens. These bromine, amino and oxygen atoms show electronegative property, so that the theoretical chemical shift of C_2, C_3, C_4, C_5 and C_6 seems to be for ABMP 158.801, 118.221, 143.513, 123.531 and 140.946 ppm. The chemical shift of C_2 is greater than the other carbon values. This increase in chemical shift is due to the substitution of more electronegative oxygen and amino atoms in the heterocyclic ring. The presence of electronegative atom attracts all electron clouds of carbon atoms towards the oxygen and amino atoms, which leads to deshielding of carbon atom and net result in increase in chemical shift value. The NMR shielding surfaces of C_4 is shown in this work the chemical shift (δ) for carbon atoms presented in the MMP and ABMP in gas phase has been studied and experimental ^{13}C, ^{1}H-NMR isotropic shielding of carbon and Hydrogen atom are shown in Fig. 5. In the NMR shielding surfaces, the blue region represents shielding and red region represents de-shielding are shown in Fig. 6. The relationship between the experimental chemical shift and computed GIAO/B3LYP/6-31++G(d,p) levels for ^{13}C are shown in Fig. 7 and ABMP, respectively.

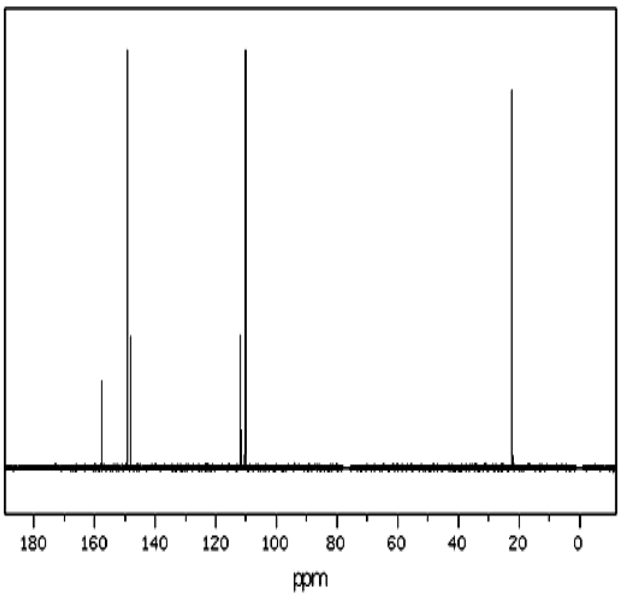

Figure 5. Observed ^{13}C NMR spectrum of 2-amino-5-bromo-4-methylpyridin

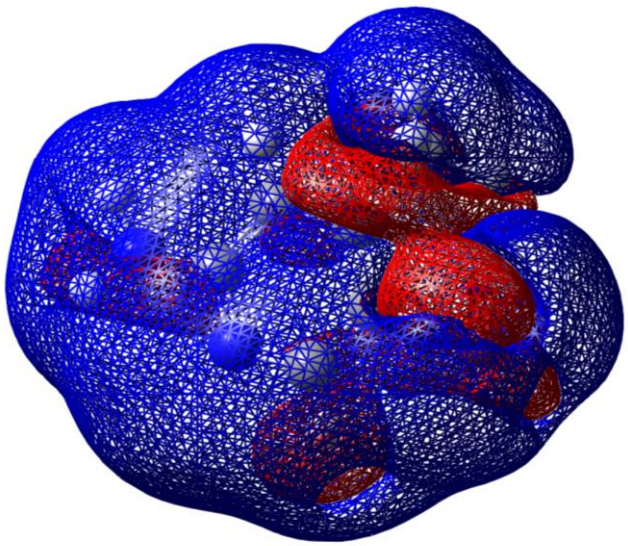

Figure 6. NMR shielding surface of 2-amino-5-bromo-4-methylpyridine

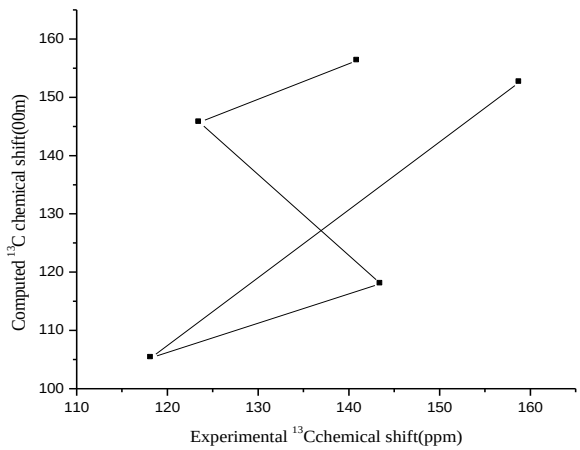

Figure 7. Computed and experimental values of 2-amino-5-bromo-4-methylpyridine

Conclusion

The optimized geometries, harmonic vibrational wave numbers and intensities of vibrational bands of 2-amino-5-bromo-4-methyl pyridine have been determined using HF/6-311+G(d,p), DFT/6-311+G(d,p) and DFT/ 6-311++G(d,p) methods and basis sets. This DFT based quantum mechanical approach provides the most reliable theoretical information on the vibrational properties of the molecules. The scaled B3LYP/6-311++G(d,p) results are the best over the other basis set. The influence of CH_3 group and the electron withdrawing nature of Br atom in the ABMP were also discussed. NMR (^1H and ^{13}C) spectral studies were carried out. The normal modes of ABMP have been studied by FTIR and FT-Raman spectroscopies. The HOMO-LUMO energy gap of ABMP calculated at the HF/311+G(d,p), DFT/6-311+G(d,p) and DFT/6-311++G(d,p) level reveals that the energy gap reflect the chemical activity of the molecule. Lower in the HOMO-LUMO energy gap explains the eventual charge transfer interactions taking place within the molecule. NBO analysis has been performed on ABMP molecule in order to elucidate intermolecular hydrogen bonding, charge transfer (CT), rehybridization, delocalization of electron density and cooperative effect due to L(N1) $\rightarrow$ σ*(C-C) for ABMP. The assignments of most of the fundamentals provided in the present investigations are believed to be unambiguous.

References

[1] T.L. Gilchrist, Heterocyclic chemistry, Addison Wesley Longman (1997).

[2] M. Okamato, K. Takahashi, T. Doi, Y. Takimoto, Anal. Chem., 69 (1997) 2919.

[3] Z. Dega-Szafran, A. Kania, B. Nowak-Wyadra, M. Szafran, J. Mol. Struct., 322 (1994) 223.

[4] P. Carmona, M. Molina, R. Escobar, Spectrochim. Acta 49A (1993) 1.

[5] S. Hildbrand, A. Blaser, S.P. Parle, C.J. Leman, J. Am. Chem. Soc., 119 (1997) 5499.

[6] D. Gandolfo, J. Zarembowitch, Spectrochim. Acta 33A (1977) 615.

[7] T.K.K. Srinivasan, J. Mol. Liquids, 26 (1983) 177.

[8] O.P. Lamba, J.S. Parihar, H.D. Bist, Y.S. Jain, Indian J. Pure Appl. Phys., 21 (1983) 236.

[9] Reena Rastogi, Ph.D. Thesis (Botony), C.C.S. Univ., Meerut (2003).

[10] R.K. Sharma, Good Manufacturing practices for ISM, Pharmaceuticals, science technology, entrepreneur, 10(18): 6(1990).

[11] NIOSH and International agency for research on cancer. IARC monographs on the evolutions of carcinogenic risks to Humans, Printing processes and Printing inks, carbon black and some Nitro compounds, Vol. 65, Lyon, Francel ARC (1996).

[12] The International pharmacopeias, Vol. 5, tests, methods and general requirements, W.H.O. Genevapub. Division (2004).

[13] Basic tests for drugs, W.H.O. Geneva - Pub. Division (2004).

[14] Official methods of analysis of the AOAC chemists, edited by K. Helrich, AOA Arlington (U.S.A.)-(2003).

[15] Official methods of microbiological analysis AOAC group, Vol. 1-3, AOAD, Arlington (U.S.A.)-(2003).

[16] The Compendium of analytical methods, Vol. 1-4, evaluation division, bureau of microbiological hazards, food directorate, Health product and food branch, Health Dept., Canada (2003).

[17] Official methods of microbiological analysis food, Vol. I, evaluation division, Health Dept., Canada (2003).

[18] Alper, Stanley, manual for therapeutics, J.W. Pub., N. York (1998).

[19] P. Pulay, G. Fogarasi, G. Pongor, J.E. Boggs, A. Vargha, J. Am. Chem. Soc. 105 (1983) 7037.

[20] M.J. Frisch, G.W. Trucks, H.B. Schlegal, GAUSSIAN 09, Revision A.02, Gaussian, Inc., Wallingford, CT, 2009.

[21] T. Sundius, J. Mol. Struct., 218 (1990) 321.

[22] T. Sundius, Vib. Spectrosc., 29 (2002) 89.

[23] MOLVIB (V.7.0): Calculation of Harmonic Force Fields and Vibrational Modes of Molecules, QCPE Program No. 807 (2002).

[24] G. Fogarasi, X. Zhou, P.W. Taylor, P. Pulay, J. Am. Chem. Soc., 114 (1992) 8191.

[25] K. Sambathkumar, Density Functional Theory Studies of Vibrational Spectra, Homo-Lumo, Nbo and Nlo Analysis of Some Cyclic and Heterocyclic Compounds (Ph.D. thesis), Bharathidasan University, Tiruchirappalli, August 2014.

[26] K.Sambathkumar,S.Jeyavijayan,M.Arivazhagan Spectrochim. Acta A 147 (2015)51-66.

[27] Kuppusamy Sambathkumar Spectrochim. Acta A 147 (2015) 51-66.

[28] R.G. Parr, L.V. Szentpaly, S.J. Liu, Am. Chem. Soc., 121 (1999) 1922.

[29] P.K. Chattraj, B. Maiti, U.J. Sarkar, J. Phys. Chem. A, 107 (2003) 4973.

[30] R.G. Parr, R.A. Donnelly, M. Levy, W.E. Palke, J. Am. Chem. Soc., 68 (1978) 3807.

[31] R.G. Parr, R.G. Pearson, J. Am. Chem. Soc., 105 (1983) 7512.

[32] *D.Cecily Mary Glory*, R.Madivanane and K.Sambathkumar *Elixir Comp. Chem. 89 (2015) 36730-36741.*

[33] Inger Nahringbauer, Ake Kvick, Acta Cryst., B33 (1977) 2902.

[34] http://riodbol.base.aist.go.jp/sdbs/(National Institute of Advanced Industrial Science).